

광바이오촉매 수소제조 시스템에의 광촉매 형태 및 미세구조의 영향에 관한 연구

이상봉, 설용건, 주현규^{†*}

연세대학교 화학공학과 & 청정기술센터, *한국에너지기술연구원 수소연료전지연구부

Study on the effect of morphology and microstructure of photocatalyst in photo/biocatalytic hydrogen production system

Sangbong Lee, Yong-gun Shul, and Hyunku Joo^{†*}

Dept. of Chem. Eng & Center for Clean Technology of Yonsei Univ.
134 Shinchon-dong, Seodaemun-ku, Seoul, Korea

*Hydrogen & Fuel Cell Research Dept., Korea Institute of Energy Research
71-2 Jang-dong, Yusong-ku, Taejeon, 305-343, Korea

ABSTRACT

이 연구는 광화학적 물분해 수소제조 기술의 일환으로 수행 중인 광촉매와 바이오촉매를 복합한 시스템 활용 기술에서 광촉매가 갖는 물리적 특성의 영향을 파악하고자 진행되었다. 다양한 물리적 특성을 갖는 광촉매를 얻기 위하여 상용광촉매, 수열화법(HT-TiON), 그리고 저온합성법(LT-TiON) 등을 이용하여 샘플을 준비하였다. 가시광 감응을 위하여 암모니아나 triethylamine 처리를 하여 질소를 도핑도 시도하였다. 시도된 복합 시스템은 인위적인 전자주개 없이 수소를 발생시키는 결과를 보여주었으나, 광촉매로부터 엔자임으로의 전자전달 부분이 율속단계로 확인되었다. 사용된 광촉매 샘플에 따라 수소 발생량에 차이가 나타난 결과로 광촉매의 미세구조(결정상, 결정도, 기공 크기 및 비표면적 등)이 중요한 역할을 하는 것으로 판단되었다. 얻어진 결과들을 활용하여 재료들이 고정화된 새로운 시스템 구성을 제안하였다.

주요기술용어 : Photocatalyst(광촉매), Enzyme(엔자임), H₂ production(수소 제조), Photobiocatalytic(광바이오촉매적), Hydrogenase(수소발생효소)

Environmental remediation using photocatalysts has been a major focus in many countries over the last decade. Also, numerous studies have been focused on hydrogen from water as a clean energy resource since the invention of

1. INTRODUCTION

[†] Corresponding author : hkjoo@kier.re.kr

photochemical water splitting over TiO_2 electrode. However, the photocatalytic process has been simultaneously criticized as being uneconomical compared to other oxidative treatment systems and hydrogen production systems due to its inherent low efficiency and limitations resulting from the necessities for an appropriate light source and immobilization, which that may increase the overall energy costs¹⁾. Therefore, there has been a great deal of interest in tackling the aforementioned key issues to economically commercialize photocatalytic systems.

As far as production of hydrogen is concerned, one of the IEA hydrogen programs (known as the Hydrogen Implementing Agreement (HIA)), Annex-14, focused on the development of materials and systems for the photoelectrochemical (PEC) production of hydrogen⁹⁾. On the other hand, in Korea one program of 21st Century Frontier R&D Program, the Hydrogen R&D Research Center, has brought together a relatively broad range of topics to address challenges with a long term global view. From hydrogenase's point of view, photo/biocatalytic system for hydrogen production

was studied previously by Russian researchers and others in early 80's, while present study has directed to photocatalytic aspect. In in vitro biological system for hydrogen production, complex electron transport systems exist such as photosystem (PS) II and I, and ferredoxin (FD). This electron transport system can be simply theoretically replaced with visible-light sensitized photocatalyst. Thus, the photocatalyst sensitized by solar irradiation produces electrons and holes (electron vacancies) which then can be separated to reduce protons and to oxidize electron donor (Fig. 1). For this visible light-activated point of view, e.g. for the photocatalyst particles to be activated by visible light, nitrogen-substituted TiO_2 (TiON) has been studied, either by sputtering or by hydrolyzing an aqueous $\text{Ti}(\text{SO}_4)_2$ solution with a NH_3 solution^{2,3)}. Moreover, the efficient charge separation is not related to absorption of light with the wavelength shorter than that of bandgap energy, but depends on the physical properties of the samples such as the shape, distribution pores, crystalline phase, crystallinity, and the preparation and the post-deposition treatments. Therefore, the effect of physical

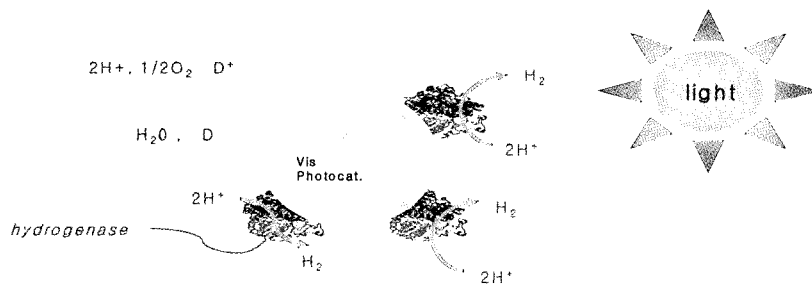


Fig. 1. Schematic view of photo/biocatalytic hydrogen production system.

properties must be considered.

In this study to prepare visible light sensitized photocatalyst potentially used in photo/biocatalytic hydrogen production system, nitrogen-substituted TiO₂ (TiON) was prepared by a hydrothermal technique. The selected TiON samples in any shape and microstructure was characterized and combined with a biocatalyst (or hydrogenase enzyme) to produce hydrogen. Various methods have been performed to correlate the ease of charge transportation to enzyme with physical properties of photocatalysts from different procedures. With collected results and decisions, novel system configurations are proposed for future works.

2. EXPERIMENTAL

Visiblelight-activated nitrogen-substituted titanium oxide (TiON) was prepared combining a couple of methods, one of them being the hydrothermal method. P25 TiO₂ (Degussa, FRG), UV100 (Hombikat, FRG) and NT22 TiO₂ (NANO Co., Ltd. Korea) were used as a raw material and a reference when necessary. In a typical preparation procedure for TiON, anatase TiO₂ powders were placed into a teflon-lined autoclave with a 50m capacity. The autoclave was then filled with a aqueous solution of NaOH with a certain molar concentration up to 80% of the total volume of the autoclave and was maintained under the desirable conditions without shaking or stirring during the heating process. Washing and drying was then performed.

To narrow the conditions the one-third fractional factorial experiment involving 9 FLC was used to reduce the size of the experiment: a full factorial experiment a 3³=27 factor-level combination (FLC) occurs when there are three

factors and three levels for each factor. The selected factors consist of the NaOH concentration (levels of 1, 3 and 5M), temperature (levels of 175, 220 and 225 °C) and time (levels of 12, 24 and 36 hr). As a preliminary experiment, raw TiO₂ for TiON was prepared using titanium tetraisopropoxide (TTIP), isopropyl alcohol (IPA), acetic acid and water for comparison. Finally, the substitution of nitrogen into the hydrothermally treated TiO₂ was performed by mixing TiO₂ powder with a NH₃ solution followed by drying (Fig. 2). LT-TiON was prepared using low temperature synthesis with triethylamine (TEA), resulting in anatase crystallite phase and ca. 170 m²/g of surface area.

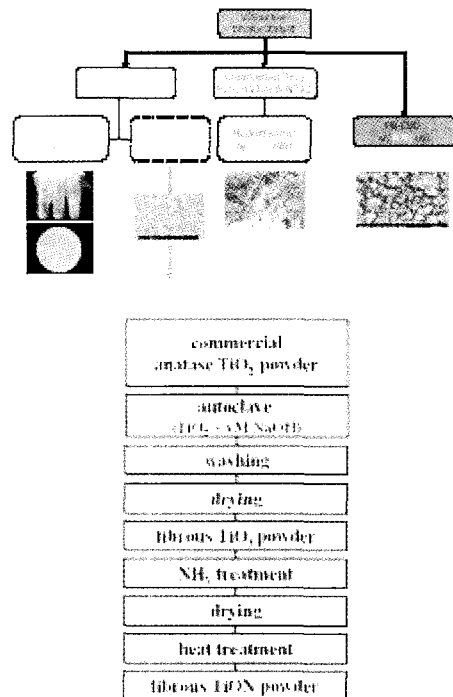


Fig. 2. Flow chart for the preparation of various photocatalysts (top) and one of procedures of HT-TiON (bottom)

Purified hydrogenase (Pyrococcus furiosus, Pfu) was purchased from Prof. Adams at the University of Georgia. Activity of Pfu was stable for at least 48 hr after it was out of a freezer. And activity assay of Pfu (21834 unit/ml) was much higher than that of Clostridium butyricum (1442 unit/ml) and Thiocapsa roseopersicine (1704 unit/ml) determined at Tris-HCl (50mM, pH 8.5, 50 °C, absorbance at 570 nm). Specific activity (unit/mg, Bio-rad protein assay, absorbance at 750 nm) of Pfu was two to three times higher than that of the latter hydrogenases. Activity was lower in phosphaste, but similar in EPPS buffer. Methyl viologen (MV), tris(hydroxymethyl)aminomethane (Tris), phosphate,

MES, sodium formate, and sodium dithionite (Na-D) were obtained from Sigma and used as received.

The light sources used were UV-A lamps (Sankyo Denki, Japan), halogen lamp and LED (green and blue peaked at 520 nm and 464 nm, respectively.). Isopropyl alcohol (IPA) was a probe compound for measuring the activity. The chemicals (IPA, acetone and CO₂) were analyzed by gas chromatography with a flame ionization detector (GC/FID, HP 5890) and a GC/FID with a methanizer (HP6890). Hydrogen production was analyzed by gas chromatograph with TCD (thermal conductivity detector at 160 °C). The used column in the system was molecular sieve 5A. Typical oven temperature was maintained at 40 °C. Moisture trap (silica-gel) was placed just before GC auto injection valve to prevent damage by water. The structure, morphology and the surface area were investigated using XRD (Rigaku, DMAX/2000-Ultima Plus), SEM (Topcon SM-720), and BET.

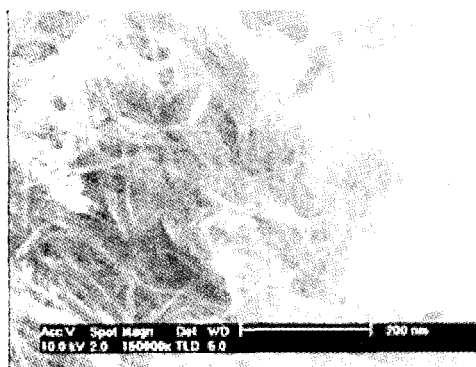


Fig. 3. SEM images of the hydrothermally prepared TiO₂ (top: 10M NaOH, 175 °C, 12 hr, bottom: with 20 vol% SiO₂ added).

3. RESULTS AND DISCUSSIONS

Initially, a rough hydrothermal experiment with NH₄OH and the prepared raw TiO₂ (189 m²/g) revealed that the sample turned a yellow color and absorbed light with wavelength < 520 nm. In addition, using aqueous NaOH (10 M) and a 12hr reaction time under varying reaction temperatures ranging from 100 ~ 200 °C, five samples (with 25 °C interval) exhibited the beta phase TiO₂ (β-TiO₂; Na₂TiO₃, Na₂Ti₃O₇) from XRD analysis with a maximum specific surface area of 246 m²/g at 175 °C. The addition of silica made the particle size more uniformly distributed (a fibrous shape was identified by SEM, Fig. 3).

Table 1. Effect¹ of the washing procedure² on the physical properties of HT-TiO₂ from NT22 under 10M NaOH, 175 °C, 12hr

	BET surface area (m ² /g)	Pore volume (cm ³ /g)	Pore radius (nm)
NT-22	64.7427	0.22792	6.82975
W0	16.0104	0.05916	7.38978
W1	164.3932	0.33846	4.11769
W2	308.8273	0.85506	5.53749
W3	308.8627	0.88443	5.72702

¹While impurity peaks dominate crystal phases in XRD analysis under W0, washing procedures (W1~W3) removes impurities, resulting in some characteristic crystal peaks. This can be also seen with drastically increasing surface area (or pore volume) in the Table 1.

²W0: without washing, W1: washing only with water, W2: washing only with HCl, W3: washing with water and HCl.

The tube shape TiO₂ using the hydrothermal method was identified and explained by Wang et al.⁵⁾, where they suggested a mechanism by which anatase TiO₂ nanotubes grow. They also reported that the nanotubes were formed during the alkali treatment, with subsequent acidic treatments having little or no effect on nanotube structure and shape. In order to investigate the effect of the washing procedure on the physical properties of selected samples (HT-TiO₂ from commercialized TiO₂ powder (NT22) under 10M NaOH, 175 °C, 12hr), four different washing procedures were performed (W0: without washing, W1: washing only with water, W2: washing only with HCl, W3: washing with water and HCl). The following properties: specific surface area, pore radius and pore volume, were changed with respect to the washing procedure used, showing a linear relationship between the specific surface area and pore radius (Table 1). XRD showed that NaOH remained on the surface without washing (W0), with the other three methods showing no difference (β -TiO₂ present). This suggests that washing is essential for removing impurities

and controlling the shape. A systematic approach for preparing the photo-active TiO₂ was made using a fractional factorial design (FFD), a tool for experimental setup. Table 2 shows the selected 9 factor-level combinations (FLCs) out of the total of 27 FLCs⁶⁾. From an analysis of the variance (ANOVA), reaction temperature had 99% level of significance on the specific surface area. The NaOH concentration of was critical to the phase formed. For example, the anatase phase was formed with 1M of NaOH, the β -phase was formed with 5M of NaOH, and the anatase was formed with below 225 °C and β -phase above 225 °C for 3M of NaOH. The specific surface area increased from 65 m²/g to 144 m²/g (5M NaOH, 225 °C, 12hr). Fig. 4 shows SEM images for selected samples, where a fibrous shape of TiO₂ was revealed at concentrations > 3M of NaOH. Detailed investigations based on the 3M NaOH, 175 °C and 12hr were examined in terms of the phase and shape, varying the NaOH concentration (3.5, 4, 4.5 M) first and then followed by altering the reaction temperature and time. The resulting optimum condition was

Table 2. Selected factor-level combinations (FLCs) and ANOVA analysis for the significant factor selection on surface area of TiON

	1M NaOH			3M NaOH			5M NaOH		
	12hr	24hr	36hr	12hr	24hr	36hr	12hr	24hr	36hr
175 °C	■				■				■
200 °C			■	■				■	
225 °C		■				■	■		
Source ^a (df)	Sum of squares (SS)			Mean square (MS)			distribution Fo		
Total (8)									
A (2)	93.639			46.819*					
B (2)	1016.992			508.496			11.71 ^b		
C (2)	34.657			17.329*					
A×B (2)	132.156			66.078*					
Residual				43.409 (6df)					

^a : A: mole of NHOH, B: Rxn temperature, C: Rxn time, * : Components involved in residuals.

^b : 0.01 level of significance.

found to be 4M of NaOH, 200 °C and 12 hr (103 m²/g).

A summary of the physical properties of the selected samples is shown in Table 3, and their photocatalytic activity in degrading IPA using UV-A irradiation is shown in Fig.5. P25 showed the fastest reaction rate, followed by NT22. The optimized sample (4M200T12-8/2w) showed a better activity than the other samples prepared, but was less active than the two commercialized TiO₂ samples under UV-A irradiation. The observed change in surface area is attributable to the crystallization of walls separating mesopores. This tendency subsequently caused an change in mean pore diameter and pore volume of the bulk materials. Consequently, the loss in surface area caused an increase in pore diameter and a decrease in pore volume⁷⁾.

The optimized sample (4M200T12-8/2w) was further analyzed by DSC to identify the heat-treatment temperature to substitute nitrogen,

where a distinguishable exothermic band appeared near 430 °C. This exothermic reaction was attributed to be the oxidation reaction of NH₃ or NH₂ with the oxygen released from the amorphous grain boundaries by forming oxygen-deficient sites³⁾. This band was not

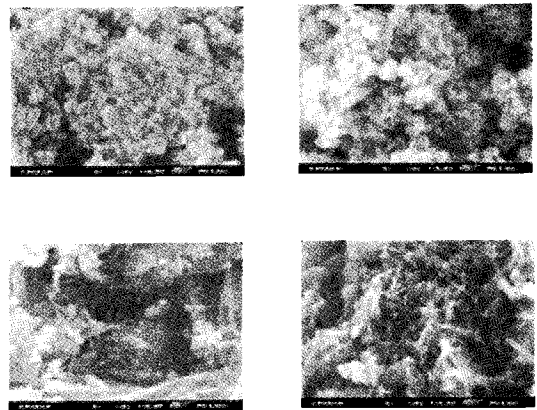


Fig. 4. SEM images of selected samples from the FFD experimental design. [(a)3M175T24, (b)3M200T12, (c)3M225T36, (d)5M175T36]

Table 3. Physical properties of the selected samples¹

	P25	NT22	4M200T12-(8/2w)SiO ₂	4M200T12	3M225T36	5M225T12
Phase	anatase+rutile	anatase	anatase	anatase	anatase+β-TiO ₂	β-TiO ₂
XRD intensity (θ)	545 (25.18)	1392 (25.16)	688 (25.30)	528 (25.26)	454 (25.26)	262 (24.26)
1/2 width	0.36	0.42	0.43	0.43	0.46	-
BET (m ² /g)	50	64.7	127.6	102.7	52.3	114.0
Pore Vol. (cm ³ /g)	-	0.228	0.448	0.365	0.189	0.566

¹Here also, same phenomena happens in XRD analysis according to washing procedures and same explanation can be applied to that in the Table 1. However, with the same washing procedure W3 obtained samples except 4M200T12 series have fairly low crystallinity. The highest one is NT22, which shows peak height twice as high as one of P25. Selected sample, 4M200T12-(8/2w)SiO₂, has similar peak height to P25.

significant due to the small amount of the amorphous portion in the obtained samples by the hydrothermal method. This fact needs to be further studied in terms of the ease and the extent of nitrogen-substitution. As a consequence, NH₃ treatment, followed by heat-treatment at 450 °C produced yellow powders (HT-TiON, Fig. 6). A commercially available blue LED (peaked at 464 nm) was used to check the photocatalytic activity of the obtained HT-TiON (Fig. 7). Acetone evolution as a function of blue LED irradiation time was remarkable for the HT-TiON sample, but no acetone was detected for the NT22 sample (P25 also revealed no acetone production in other study by authors, data not shown)

To obtain the direct insights for photo/biocatalytic hydrogen production system, two sets of one-third fractional factorial experiment involving 9 FLC was used in order to reduce the size of the experiment: a full factorial experiment 3³=27 factor-level

combination (FLC) when three factors and three levels for each factor. The factors considered included species of buffer solution, the amount of hydrogenase (Pfu), electron donor, reaction temperature and electron mediator. The correlation of electron mediator and Pfu was also studied by a half of 24 design (8 FLCs). For a fixed hydrogenase (Pfu), four factors CdCl₂, Na-dithionite, sodium formate and MV was tested in terms of presence (two levels) in a designed manner. The results from the ANOVA showed that the amount of Pfu and Pfu+species of buffer were significant at the 0.25 significance level for the H₂ production. And Pfu+pH of Tris was significant at the 0.1 significance level and each of factor A and B were significant at the 0.025 significance level for the H₂ production. The two-factor interactions showed significant effect on the response variables (Table 4). Using two commercial samples (P25 & UV100) and two prepared ones (low temperature synthesis; LT, hydrothermal

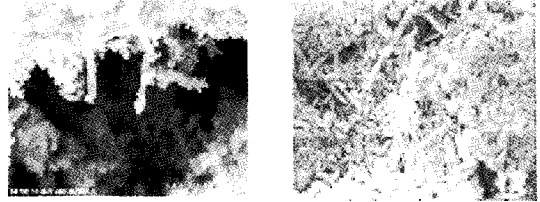
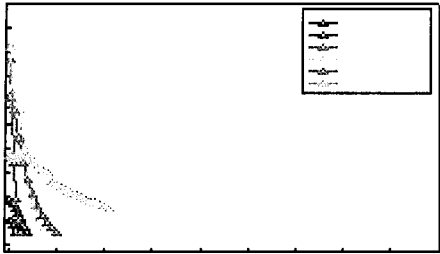


Fig. 6. SEM images of optimized 4M200T12-8/2w after the NH₃ treatment (HT-TiON).

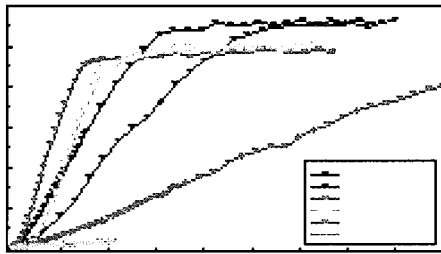
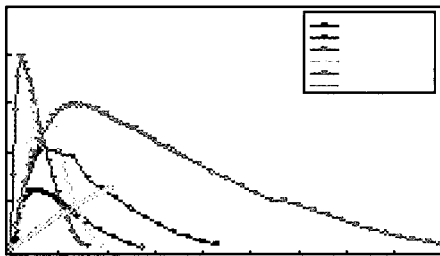


Fig. 5. Photocatalytic IPA degradation using selected samples (UV-A lamp, 840 ml reactor, IPA=38 mol, 0.15g of photocatalyst).

treatment, HT), experiments for photo/biocatalytic hydrogen production was conducted just to see how well the system works, sequential works in details are planned, though. It can be generally said that mentioned photo/biocatalytic system is described as a possible candidate for hydrogen production technique with solar irradiation. The difference in evolution rate suggested the extent

and the direction of research to be performed (Fig. 8). Rough photonic efficiency was calculated as follows.

$$\phi = \frac{K_{H_2}}{K_{irr}}$$

where K_{H_2} denotes the amount of produced H₂ in mol/s and K_{irr} irradiated light in mol (photon)/s.

$$K_{irr} = \int \frac{I}{U_{\lambda}} d\lambda = \int \frac{I \times \lambda}{hcN_A} d\lambda$$

Here, I represents measured light intensity [W], h Plank constant [6.6260755×10⁻³⁴ Js], c speed of light in vacuum [3×10⁸ m/s], N_A :

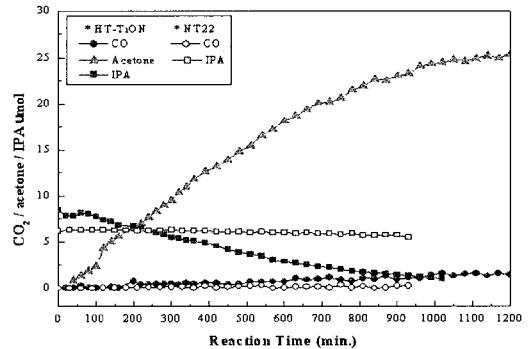


Fig. 7. Photocatalytic IPA degradation using HT-TiON and NT22. (blue LED, 840 ml reactor, IPA 38 μmol, photocatalyst 0.15g)

Avogadro number [$6.0221367 \times 10^{23} \text{ mol}^{-1}$] and representative wavelength of irradiated light [386 nm]. Measured total intensity I was ca. 700 W per cm^2 (between 310 ~ 386 nm UV range of used halogen lamp. This measured value is about one fifth of solar irradiation on earth, $3 \sim 4 \text{ mW/cm}^2$). Hence, resulted K_{irr} turned out $20.3 \times 10^{10} \text{ mol photon/s}$. According to a reference, solar irradiation is $1.5 \times 10^6 \text{ mol/s per } 1.4245 \times 10^2 \text{ m}^2$ in terms of mol photon/s^8 , which means $105 \times 10^{10} \text{ mol photon/s per cm}^2$. This is also five times higher than measured intensity I . As a result, with 20mg of photocatalyst approximately $5.6 \times 10^{10} \text{ mol H}_2/\text{s}$ produced. Therefore, rough photonic efficiency was close to 30%.

Figure 9 shows the schematic view of summarized reaction mechanism where electrons transfer from photocatalyst to relay chemical was identified as a rate determining step. As a result, factors to be considered for the next progress were selected as follows. One is to separate photocatalyst and hydrogenase to

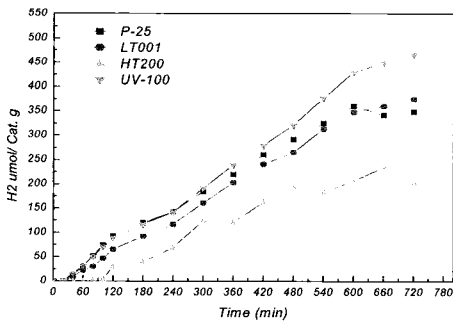


Fig. 8. Photo/biocatalytic hydrogen production (halogen lamp: UV 700 W/cm², Pfu 0.1 ml (ca. 0.35 unit=1g) and 20 mg of photocatalyst in EPPS buffer at pH 8.0 with MV 2.5 mM).

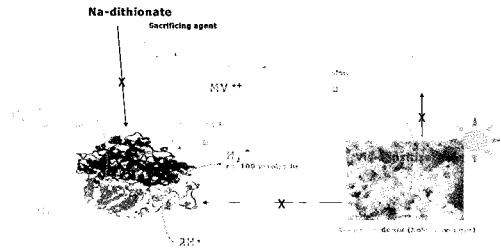


Fig. 9. Schematic view of the mechanism for photo/biocatalytic hydrogen production system.

overcome barriers such as instability of hydrogenase to photon and back reaction of hydrogen to water. Second is from system's point of view to immobilize photocatalyst and hydrogenase, which consequently prevents deactivation and enhances durability. Thirdly, it should be taken into account to replace reaction media with "useful" wastes streams that match to the requirements. Current results initiated the tentative decision on system configuration for future works as shown in Fig. 10 where proton exchange membrane or ionic conductor separates

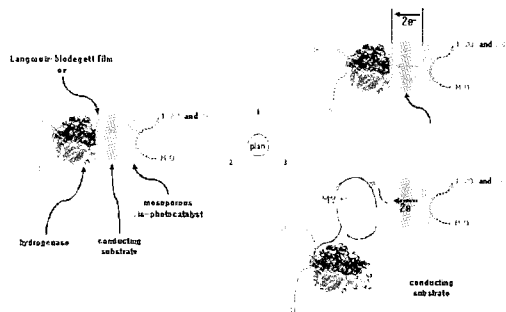


Fig. 10. Proposed reactor configuration for photo/biocatalytic hydrogen production system.

Table 4. Results from factor-level combinations of reaction condition. Step 1: A=Pfu (Level 0= 0, 1=0.3, 2=0.6 Unit); B=Buffer (0=MES, 1=Tris, 2= Phosphate); C=Na-dithionite, 230 mM (0=0, 1=0.1, 2=0.2 ml), Step 2: A=MV (Level 0= 0, 1=1.5, 2=2.5 mM); B=Tris (0=pH 7, 1=pH 8, 2= pH 9); C=Reaction Temp.(0=50, 1=60, 2=70 oC)

Factor & Level			Step 1 (H ₂ μmol, after 120 min)	Step 2 (H ₂ μmol, after 120 min)
A	B	C		
0	0	0	0	0.28
0	1	2	0	1.052
1	0	1	4.107	0.949
2	0	2	5.493	0.69
0	2	1	0	0.652
1	1	0	0	3.981
1	2	2	2.17	14.628
2	1	1	11.403	7.814
2	2	0	0	6.885

sensitizer and enzyme which can be immobilized with Langmuir-Blodegett film.

4. CONCLUSION

For hydrogen production with solar irradiation, a relatively novel approach was started where sensitized photocatalysts give electrons to hydrogenase that reduces protons into hydrogen. While doing the research, this study was planned, investigated examining the possible role of morphology and microstructure of photocatalyst in photo/biocatalytic hydrogen production system. With the a limited loss in the reduction potential, nitrogen-substituted TiO₂ can theoretically act asplaya major role in visible light activation only with the efficient charge carriers' separation achieved. Structural modification of material turns out important, but not optimized up to now mainly because of poor charge separation. The high crystallinity seems

to be the most necessary factor among considered. As a result, testing a large number of photocatalysts, immobilization of reaction constituents was planned to perform in parallel.

후 기

This research was performed for the Hydrogen Energy R&D Center, one of the 21st Century Frontier R&D Program and partly for KIER project, both funded by the Ministry of Science and Technology of Korea.

참 고 문 헌

- 1) Raupp GB, Alexiadis A, Hossain M, Changrani R., Catalysis Today, 69, 2001, 41-42.
- 2) Ashai R, Morikawa T, Ohwaki T, Aoki K, Taga Y., SCIENCE, 293, 2001, 269-271.
- 3) Ihara T, Miyoshi M, Iriyama Y, Matsumoto O, Sugihara S., Applied Catalysis B: Environmental, 42, 2003, 403-409.

- 4) Morey, G. W., Niggli, P., J. Am. Chem. Soc., 35, 1913, 1086-1130.
- 5) Wang, W., Varghese, O. K., Paulose, M., Grimes, C. A., Wang, Q., Dickey, E. C., J. Mater. Res., Vol. 19, No. 2, 2004, 420-421.
- 6) D. C. Montgomery: "Design and Analysis of Experiments", John Wiley & Sons, USA. 1991.
- 7) Sreethawong, T., Suzuki, Y., Yoshikawa, S., J. of Solid State Chemistry 178, 2005, 329-338.
- 8) Ljubas, D., Energy 30, 2005, 1699-1710.
- 9) Andreas Luzzi ed. "Photoelectrolytic production of hydrogen, IEA Hydrogen Program, Annex-14", Final report, 2004.